Quasiparticle excitation spectrum for nearly-free-electron metals

John E. Northrup
Xerox Corporation, Palo Alto Research Center, 3333 Coyote Hill Road, Palo Alto, California 94304

Mark S. Hybertsen
AT&T Bell Laboratories, 600 Mountain Avenue, Murray Hill, New Jersey 07974-2070

Steven G. Louie
Department of Physics, University of California, Berkeley, California 94720
and Materials and Molecular Research Division, Lawrence Berkeley Laboratory, Berkeley, California 94720
(Received 21 December 1988)

The quasiparticle excitation spectrum is calculated for the nearly-free-electron metals Li, Na, and Al by evaluation of the electron self-energy operator within the GW approximation and a generalized plasmon-pole model. The calculated quasiparticle energies for Na and Al are in excellent agreement with angle-resolved photoemission experiments. For Na in particular, the occupied-band width is significantly narrower than the free-electron value, as found in experiment. Inclusion of exchange and correlation effects in the dielectric matrix is shown to decrease the bandwidth relative to the random-phase-approximation result by a significant amount. Local-field effects, reflected in the off-diagonal elements of the dielectric matrix, are found to have little effect on the quasiparticle band structure of these simple metals.

I. INTRODUCTION

Most modern band-structure calculations are based on some form of local-density-functional theory together with the assumption that the Kohn-Sham[1] eigenvalues can be interpreted as the energy required to add or remove an electron from an infinite solid. Although this approach for obtaining excitation energies is without a rigorous theoretical foundation, in practice it has been very useful in unraveling the essential physics in many condensed-matter systems. However, it is well known that this approach fails to give band gaps correctly in semiconductors and insulators. It systematically underestimates the magnitude of the energy gap.[2] Less well known is the fact that the local-density-approximation (LDA) eigenvalues overestimate the valence-band width of simple metals such as Na, Mg, and Al.[3]

Achieving a better predictive capability for solid-state electronic properties requires a theory specifically designed to yield the energies of the excited states. Such a theory must treat accurately both the many-particle correlation effects and the one-body crystalline potential. Recently, there has been considerable progress in this direction. For example, it has been demonstrated that the band gaps of semiconductors and insulators can be calculated to an accuracy of ~ 0.1 eV provided that the nonlocality and energy dependence of the self-energy operator are treated properly.[4,5]

In this paper we report calculations of the electronic excitation energies for the metals Na, Li, and Al. The calculations are based on Hedin's GW approximation,[6,7] wherein the electron self-energy operator is approximated by the first term in a perturbative expansion in powers of the screened Coulomb interaction and the dressed electron Green function.

Because Na is a nearly-free-electron metal with a simple valence-band structure, it can be used as a testing ground for theories of many-body effects in electronic structure. Angle-resolved photoemission experiments[8,9] for Na indicate that the occupied valence band is almost parabolic in shape and has an energy width of 2.5–2.65 eV. These results are consistent with earlier x-ray photoemission data.[10] The measured bandwidth is significantly less than the free-electron value, 3.21 eV, and the value obtained in local-density calculations, 3.16 eV. The lack of agreement between these theoretical estimates and the experimental values has its origin in the inadequate treatment of electronic correlations. From Hedin's work it is known that dynamical correlation effects tend to reduce the bandwidth.[6,7] Hedin's calculations for the electron gas, which employed the GW approximation and random-phase-approximation (RPA) dielectric screening, indicated a bandwidth reduction of about 10% for the electron gas with the same electron density as Na. This reduction is not enough to account for the experimental result. The apparent failure of the existing many-body perturbation theory to account for the bandwidth observed in Na has resulted in several new approaches.[11,12] We have demonstrated recently[12] that, for Na, excellent agreement with experiment can be obtained within the GW approach if exchange-correlation effects are included in the calculation of the dielectric function determining the screened Coulomb interaction.

The rest of this paper is organized as follows. In Sec. II the underlying theory is outlined. In Sec. III we discuss the details of the numerical calculations. Results for the metals Na, Li, and Al are given in Sec. IV, and Sec. V contains an analysis of the results in terms of electron-gas calculations.

II. THEORY

The method used here to calculate excitation energies is based on many-body perturbation theory and employs Green-function techniques. The underlying theory has been reviewed extensively in Ref. 7. A detailed discussion of the calculational procedure can be found in Ref. 4. In the Green-function approach the particlelike electronic excitation energies of a many-electron system are given by the eigenvalues $E_{n\mathbf{k}}$ of the quasiparticle equation:

$$[T+V_{\rm ext}(\mathbf{r})+V_H(\mathbf{r})]\Psi(\mathbf{r}) + \int \Sigma(\mathbf{r},\mathbf{r}';E_{n\mathbf{k}})\Psi(\mathbf{r}')d\mathbf{r}'=E_{n\mathbf{k}}\Psi(\mathbf{r}) . \quad (1)$$

In this equation T is the electron kinetic-energy operator, $V_{\rm ext}(\mathbf{r})$ is the electron-ion interaction, $V_H(\mathbf{r})$ is the Hartree potential, and Σ is the self-energy operator. The main problem lies in determining Σ. Because Σ is not necessarily Hermitian, the eigenvalues $E_{n\mathbf{k}}$ of the quasiparticle equation are, in general, complex; the real part determines the energy of the excited state and the imaginary part determines the lifetime. In the present work we retain only the real part of the self-energy operator in the quasiparticle equation. Consequently, the eigenvalues $E_{n\mathbf{k}}$ are real and correspond to quasiparticle excitations with infinite lifetime.

The self-energy operator is written as

$$\Sigma(\mathbf{r},\mathbf{r}';E)=(i/2\pi)\int G(\mathbf{r},\mathbf{r}';E+\omega)W(\mathbf{r},\mathbf{r}';\omega)e^{i\delta\omega}d\omega , \quad (2)$$

where G is the dressed electron Green function and W is the screened Coulomb interaction. This is the first-order term in a perturbation expansion of the self-energy. Vertex corrections are neglected. W can be expressed in terms of the bare Coulomb interaction and the time-ordered dynamical dielectric function:

$$W(\mathbf{r},\mathbf{r}';\omega)=\int \epsilon^{-1}(\mathbf{r},\mathbf{r}'';\omega)v(\mathbf{r}''-\mathbf{r}')d\mathbf{r}'' . \quad (3)$$

Once G and W are known, the self-energy operator can be obtained and the quasiparticle equation solved. Here, a quasiparticle approximation is used for G:

$$G(\mathbf{r},\mathbf{r}';\omega)=\sum_{n,\mathbf{k}}\Psi_{n\mathbf{k}}(\mathbf{r}) \times\Psi^*_{n\mathbf{k}}(\mathbf{r}')/[\omega-E_{n\mathbf{k}}-i\delta\,\mathrm{sgn}(E_F-E_{n\mathbf{k}})] . \quad (4)$$

The screened Coulomb interaction is determined by the dynamic dielectric function. For a crystal, calculation of $\epsilon^{-1}(\mathbf{r},\mathbf{r}';\omega)$, or, in reciprocal space, $\epsilon^{-1}_{\mathbf{G},\mathbf{G}'}(\mathbf{q},\omega)$, for all ω is a formidable task which we circumvent by use of a generalized plasmon-pole approximation.[4] In the plasmon-pole model, for each matrix element of ϵ^{-1}, we postulate the following simple analytic form:

$$\epsilon^{-1}_{\mathbf{G},\mathbf{G}'}(\mathbf{q},\omega)=\delta_{\mathbf{G},\mathbf{G}'}+A_{\mathbf{G},\mathbf{G}'}(\mathbf{q})[\omega-\tilde{\omega}_{\mathbf{G},\mathbf{G}'}(\mathbf{q})+i\delta]^{-1} - A_{\mathbf{G},\mathbf{G}'}(\mathbf{q})[\omega+\tilde{\omega}_{\mathbf{G},\mathbf{G}'}(\mathbf{q})+i\delta]^{-1} . \quad (5)$$

The matrices $A_{\mathbf{G},\mathbf{G}'}(\mathbf{q})$ and $\tilde{\omega}_{\mathbf{G},\mathbf{G}'}(\mathbf{q})$ are determined by the requirements that the generalized f-sum rule and the Kramers-Kronig relation be satisfied.[4] δ is a positive infinitesimal. In this model only the static dielectric matrix and the electronic charge density for the crystal are required to determine A and $\tilde{\omega}$.

The static dielectric function is defined as the functional derivative of the average electrostatic potential, the potential experienced by a test charge probe, with respect to an external potential. It is a ground-state property and can be calculated exactly, in principle, within the density-functional theory (DFT). The change in the average electrostatic potential depends on the charge density induced by the external perturbation. In DFT the induced charge density depends on the total potential (external potential plus Hartree potential plus exchange-correlation potential) induced by the external perturbation. In the DFT, linear-response theory implies that the inverse static matrix is given by

$$\epsilon^{-1}=1+v[1-P(v+K_{\rm xc})]^{-1}P , \quad (6)$$

where v is the bare Coulomb interaction, P is the independent-particle polarizability, and $K_{\rm xc}$ is the functional derivative of the exchange-correlation potential[13] with respect to the charge density,

$$K_{\rm xc}(\mathbf{r},\mathbf{r}')=\delta V_{\rm xc}(\mathbf{r})/\delta n(\mathbf{r}') . \quad (7)$$

$K_{\rm xc}$ includes the effect of exchange and correlation. The correct $K_{\rm xc}$ is not known, but in the LDA $K_{\rm xc}$ is given by

$$K_{\rm xc}(\mathbf{r},\mathbf{r}')=\{\partial V_{\rm xc}[n(\mathbf{r})]/\partial n\}\delta(\mathbf{r}-\mathbf{r}') . \quad (8)$$

The validity of this local approximation, in which $K_{\rm xc}$ is independent of $\mathbf{q}$, is explored in calculations for the electron gas described in Sec. V. Setting $K_{\rm xc}=0$ in Eq. (6) results in the RPA dielectric function. Thus, the RPA corresponds to neglecting exchange and correlation effects in calculating the total potential induced by the external potential.

We have emphasized the importance of including exchange and correlation effects in the dielectric function when calculating the self-energy for the alkali metals.[12] For the semiconductors and insulators, on the other hand, the RPA dielectric function gives very good results and the inclusion of exchange and correlation effects in the screening has a rather small effect on the band gaps. For Si the inclusion of exchange and correlation effects in the dielectric function alters the quasiparticle energies by less than 0.1 eV in the static COHSEX (Coulomb-hole plus screened-exchange) approximation of Hedin.

We should emphasize that the plasmon-pole model is especially useful when attempting to go beyond the RPA dielectric screening because a detailed theory of the ω dependence for the exact $K_{\rm xc}$ is not known. It is, of course, the exact dielectric function which should satisfy the generalized f-sum rule.[4]

In principle Σ, W, and the vertex function Γ are related by a coupled set of integral equations.[6,7] The manner in which these equations are decoupled is very important. In principle, we have employed different approximations for the vertex function Γ in the expressions for W and Σ. The justification of this decoupling procedure has been discussed by Strinati *et al.*[14]

III. CALCULATIONAL PROCEDURE

The calculation begins with a LDA (Ref. 15) first-principles pseudopotential calculation of the band structure. The pseudopotentials employed here are generated with the Kerker method.[16] The Kohn-Sham equations are solved in a plane-wave basis[17] containing waves with kinetic energies up to 8 Ry for Li and Na and 11 Ry for Al. The spatial dependence of the electron Green function and the polarizability is determined by the wave functions obtained in these calculations.

For each metal the static independent-particle polarizability matrix $P_{\mathbf{G},\mathbf{G}'}(\mathbf{q})$ was calculated on a grid containing 29 $\mathbf{q}$ points in the irreducible wedge of the first Brillouin zone (BZ). The static LDA polarizability can be expressed in terms of matrix elements between occupied and empty states;

$$P_{\mathbf{G},\mathbf{G}'}(\mathbf{q})=\sum_{n,m}\sum_{\mathbf{k}}\langle n,\mathbf{k}|e^{-i(\mathbf{q}+\mathbf{G})\cdot\mathbf{r}}|m,\mathbf{k}+\mathbf{q}\rangle\langle m,\mathbf{k}+\mathbf{q}|e^{i(\mathbf{q}+\mathbf{G}')\cdot\mathbf{r}}|n,\mathbf{k}\rangle[f(\varepsilon_{m,\mathbf{k}+\mathbf{q}})-f(\varepsilon_{n,\mathbf{k}})]/(\varepsilon_{m,\mathbf{k}+\mathbf{q}}-\varepsilon_{n,\mathbf{k}})\ . \tag{9}$$

Here $|n,\mathbf{k}\rangle$ denotes the wave function for the nth band with Bloch wave vector $\mathbf{k}$, and $f(\epsilon_{n,\mathbf{k}})$ is the occupation number of that state. The calculation of $P_{\mathbf{G},\mathbf{G}'}$, for each $\mathbf{q}$, requires an integration of $\mathbf{k}$ over the Brillouin zone. This integration is performed by performing a weighted sum over special points.[18] For Li and Na, 140 points in the irreducible wedge of the first BZ are summed over, while, for Al, 408 points are included. Calculations employing smaller sets gave quasiparticle energies which were essentially identical to the results obtained with the larger set. Table I compares test results obtained for Al with various integration sets.

The energy-dependent matrix element

$$\langle n,\mathbf{k}|\Sigma(\mathbf{r},\mathbf{r}',E)|n,\mathbf{k}\rangle$$

of the nonlocal self-energy operator Σ can be written in the following form,[4]

$$\langle n,\mathbf{k}|\Sigma(\mathbf{r},\mathbf{r}',E)|n,\mathbf{k}\rangle=\sum_{m}\sum_{\mathbf{q}}\sum_{\mathbf{G},\mathbf{G}'}\langle n,\mathbf{k}|e^{i(\mathbf{q}+\mathbf{G})\cdot\mathbf{r}}|m,\mathbf{k}-\mathbf{q}\rangle\langle m,\mathbf{k}-\mathbf{q}|e^{-i(\mathbf{q}+\mathbf{G}')\cdot\mathbf{r}}|n,\mathbf{k}\rangle$$
$$\times[S^{\mathrm{SX}}_{\mathbf{G},\mathbf{G}'}(\mathbf{q};E-\varepsilon_{m,\mathbf{k}-\mathbf{q}})f(\varepsilon_{m,\mathbf{k}-\mathbf{q}})+S^{\mathrm{CH}}_{\mathbf{G},\mathbf{G}'}(\mathbf{q};E-\varepsilon_{m,\mathbf{k}-\mathbf{q}})]\ . \tag{10a}$$

In this expression (SX denotes screened exchange, CH Coulomb hole),

$$S^{\mathrm{SX}}_{\mathbf{G},\mathbf{G}'}(\mathbf{q},\omega)=-\{\delta_{\mathbf{G},\mathbf{G}'}+\Omega^2_{\mathbf{G},\mathbf{G}'}(\mathbf{q})/[\omega^2-\tilde{\omega}^2_{\mathbf{G},\mathbf{G}'}(\mathbf{q})]\}v(\mathbf{q}+\mathbf{G}')\ , \tag{10b}$$

$$S^{\mathrm{CH}}_{\mathbf{G},\mathbf{G}'}(\mathbf{q},\omega)=\tfrac{1}{2}(\Omega^2_{\mathbf{G},\mathbf{G}'}(\mathbf{q})/\{\tilde{\omega}_{\mathbf{G},\mathbf{G}'}(\mathbf{q})[\omega-\tilde{\omega}_{\mathbf{G},\mathbf{G}'}(\mathbf{q})]\})v(\mathbf{q}+\mathbf{G}')\ . \tag{10c}$$

The matrices $\Omega_{\mathbf{G},\mathbf{G}'}(\mathbf{q})$ and $\tilde{\omega}_{\mathbf{G},\mathbf{G}'}(\mathbf{q})$ depend only on the crystalline charge density and the static dielectric matrix (see Ref. 4). Evaluation of this expression requires a summation over all $\mathbf{q}$ in the first Brillouin zone, a double sum over $\mathbf{G}$ and $\mathbf{G}'$, and a sum over bands m. The sum over $\mathbf{q}$ is accomplished by performing a weighted sum over a discrete set. The number of $\mathbf{q}$ points needed in the set to obtain reliable quasiparticle energies was determined by the following test: The self-energy operator was evaluated in an approximation where local fields are neglected (i.e., only the terms with $\mathbf{G}=\mathbf{G}'$ are included in the sum) and the diagonal elements of the static dielectric matrix are given by the Lindhard dielectric function corresponding to the appropriate electron density. The electron Green function was obtained from the LDA pseudopotential calculation. Table II contains the results obtained with this approach for the various quasiparticle energies in Al as a function of the number of $\mathbf{q}$ in the set. Clearly, the results are very insensitive to N_q over the range from $N_q=8$ to $N_q=104$. The fluctuations in the quasiparticle energy differences are of the order of 0.01 eV, and so we conclude that the set containing 29 $\mathbf{q}$ points will give reliable results in the full calculations employing the actual crystalline dielectric function and including local-field effects. The summations over reciprocal-lattice vectors $\mathbf{G}$ and $\mathbf{G}'$ include all $\mathbf{G}$ for which $|\mathbf{q}+\mathbf{G}|<G_{\max}$. For Na and Li we found $G_{\max}=2.0$ to be adequate. For Al, $G_{\max}=2.6$ was sufficient to obtain a reliable quasiparticle band structure. The sum over unoccupied bands was truncated at $N=36$ for Na and Li and at $N=46$ for Al.

TABLE I. Test results obtained for quasiparticle energy differences (in eV) for Al with several different $\mathbf{k}$-point sets employed in the Brillouin-zone integration for $P_{\mathbf{G},\mathbf{G}'}(\mathbf{q})$ [Eq. (9)]. These results were obtained with the LDA dielectric function and the LDA energy spectrum in the Green function.

	Number of $\mathbf{k}$ points		
	28	145	408
$E_{\Gamma_1}-E_{X'_4}$	7.23	7.24	7.24
$E_{X_1}-E_{X'_4}$	1.41	1.41	1.41

TABLE II. Test of convergence for the number of **q** points, $N_{\mathbf{q}}$, included in the calculation of the self-energy operator for Al [Eq. (10)]. The calculation employs the electron-gas RPA dielectric function and a crystalline Green function for Al. Energy differences are given in eV.

	Number of **q** points			
	8	29	72	104
$E_{\Gamma_1}-E_{L_2'}$	6.08	6.07		6.06
$E_{L_2'}-E_{L_1}$	0.23	0.24		0.24
$E_{\Gamma_1}-E_{X_4'}$	7.79	7.67	7.67	7.67
$E_{X_4'}-E_{X_1}$	1.45	1.43	1.43	1.42
$E_{\Gamma_1}-E_{W_3}$	9.82	9.81	9.80	
$E_{X_1}-E_{W_3}$	0.68	0.70	0.70	

Rather than solve Eq. (1) directly, a perturbative approach is adopted. We solve Eq. (1) to first order in the difference between the self-energy operator Σ and the LDA exchange-correlation potential V^{xc}. The zeroth-order solution is the Kohn-Sham eigenvalue $\epsilon_{n\mathbf{k}}$ and corresponding eigenfunction $|n\mathbf{k}\rangle$. The self-energy operator is energy dependent and must be evaluated at the quasiparticle energy $E_{n\mathbf{k}}$. With the assumptions that the energy dependence of the matrix element $\Sigma_{n\mathbf{k}}(E)=\langle n\mathbf{k}|\Sigma(E)|n\mathbf{k}\rangle$ is linear for E near $E_{n\mathbf{k}}$ and that $E_{n\mathbf{k}}\approx\varepsilon_{n\mathbf{k}}$, we obtain the first-order solution,

$$E_{n\mathbf{k}}=\epsilon_{n\mathbf{k}}+Z_{n\mathbf{k}}[\Sigma_{n\mathbf{k}}(\varepsilon_{n\mathbf{k}})-V^{\mathrm{xc}}_{n\mathbf{k}}]\ . \tag{11}$$

Here, $V^{\mathrm{xc}}_{n\mathbf{k}}$ is the matrix element of the LDA exchange-correlation potential and $Z_{n\mathbf{k}}$ is the renormalization constant,

$$Z_{n\mathbf{k}}=[1-(\partial\Sigma/\partial E)|_{E=\varepsilon_{n\mathbf{k}}}]^{-1}\ . \tag{12}$$

The excitation spectrum entering the Green function in the self-energy operator should be the quasiparticle spectrum. Initially, we employ the LDA spectrum but, subsequently, we replace it with one which closely approximates the quasiparticle spectrum. We found that to a good approximation the Kohn-Sham eigenvalues and the quasiparticle energies are related to each other in a linear fashion. This is apparent in Fig. 1 (see text below).

IV. RESULTS FOR Li, Na, AND Al METALS

Self-energy calculations were carried out for Li in the bcc structure. The volume of the unit cell was taken to be 143.617 a.u.^{3}, corresponding to an average r_s of 3.25. [In terms of the electron density n, $r_s=(3/4\pi n)^{1/3}$.] The LDA calculation gives an occupied bandwidth of 3.45 eV. The calculated quasiparticle bandwidth is 2.84 eV. The self-energy correction reduces the dispersion from Γ to N in the Brillouin zone from 3.72 to 3.09 eV, and the energy gap between the first and second bands at N is reduced from 2.83 to 2.39 eV. Thus, on average, the LDA band structure is simply compressed by about 15% when the self-energy correction is included. To our knowledge, the only experimental information pertaining to the valence-band electronic structure of Li is the soft-x-ray–emission data obtained by Crisp and Williams.[19] On the basis of these measurements, the occupied valence-band width was estimated to be 3.0 eV. This is in good agreement with our result. An experimental determina-

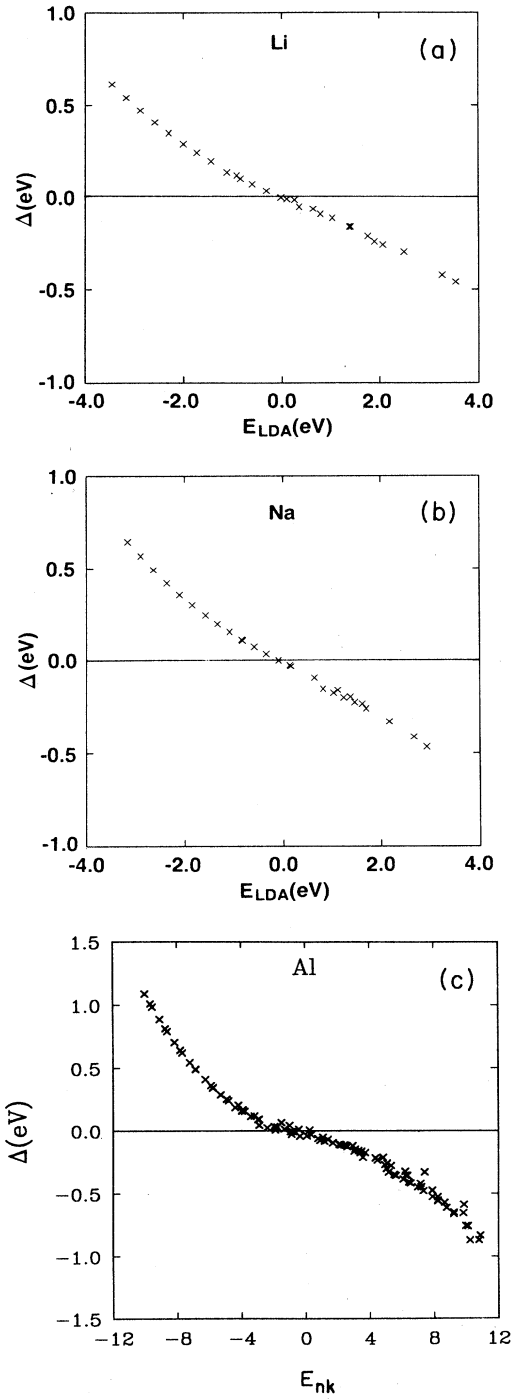

FIG. 1. Self-energy correction $\Delta=E_{n\mathbf{k}}-\varepsilon_{n\mathbf{k}}$ plotted vs LDA energy $\varepsilon_{n\mathbf{k}}$ for (a) Li and (b) Na. In (c) Δ for Al is plotted as a function of the quasiparticle energy $E_{n\mathbf{k}}$. The LDA and quasiparticle spectra are aligned at $E_F=0$.

tion of the Li band structure would be of considerable interest.

For Na we used a bcc cell with volume 258.504 a.u.^{3}, which corresponds to an r_s of 3.95. We obtain a LDA bandwidth of 3.16 eV. When self-energy corrections are included, the bandwidth is reduced to 2.52 eV. The dispersion for Γ to N is reduced from 3.98 to 3.18 eV. The width of the unoccupied part of the band between the Fermi energy and the N point is reduced from 0.82 to 0.67 eV. A photoemission experiment by Jensen and Plummer[8] indicated a Na bandwidth of 2.5±0.1 eV. A more recent photoemission experiment by Lyo and Plummer[9] indicates a bandwidth of 2.65±0.05 eV. These values are consistent with an earlier estimate based on angle-integrated x-ray-photoemission experiments.[10] Our result for the bandwidth, 2.52 eV, is in excellent agreement with the available experimental data. Recently, x-ray-absorption experiments by Citrin *et al.*[20] have indicated a 16% contraction in the width of the unoccupied part of the spectrum just above E_F. Our calculation predicts an 18% reduction.

The calculations for Al were carried out in a fcc unit cell with a volume of 112.010 a.u.^{3}, corresponding to an r_s of 2.07. Results were obtained for the first four bands at 29 points inside the irreducible wedge of the first BZ. We compare the calculated quasiparticle energies with experimental values determined in an angle-resolved photoemission experiment by Levinson *et al.*[21] in Table III. Overall, the agreement between experiment and theory is very good. There is, however, one discrepancy. Our calculations place the X_1 level at -1.51 eV below the Fermi level, while the photoemission experiment places it at -1.15 eV. On the other hand, the X_4', Z_1, Z_3, and W_3 points are all found to be within 0.1 eV of the experimental energies.[22] As a result of the difference in the placement of the X_1 level, the experimental energy gap, E_{X_1}-$E_{X_4'}$, is 1.68 eV, whereas the corresponding gap in the quasiparticle spectrum is only 1.38 eV. Another consequence of the disagreement in the energy of the X_1 level is the relative energies of the X_1 and W_3 points. The experimental result is a 0.25-eV difference in energies; the theoretical result is a 0.64-eV difference. The origin of this difference between theory and experiment remains unclear to us at this time. Analysis of the theoretical results in Tables I and II indicates that the values for the E_{X_1}-$E_{X_4'}$ energy gap and the E_{X_1}-E_{W_3} energy are both rather insensitive to the approximations involved in the momentum-space integrations. Possible sources of uncertainty in the experimental determination of the X_1 level were discussed by Levinson and co-workers.[21]

TABLE III. Quasiparticle energies in eV calculated for Al, relative to E_F, compared to experimental angle-resolved photoemission results of Levinson *et al.* (Ref. 21).

	Quasiparticle	Experiment
E_{X_1}	−1.51	−1.15
$E_{X_4'}$	−2.89	−2.83
E_{Z_1}	−1.00	−0.95
E_{Z_3}	−2.39	−2.4
E_{W_3}	−0.87	−0.90
$E_{W_2'}$	0.25	
E_{W_1}	0.90	
$E_{L_2'}$	−4.39	−4.55
E_{Γ_1}	−10.01	−10.6

In general, our results for Al are consistent with a weak pseudopotential model of the Al band structure. Pseudopotential parameters $V(200)=0.72$ eV and $V(111)=0.16$ eV can be obtained by fitting the W-point energies in a four-plane-wave model. In this model the energy gap at X is just twice $V(200)$, or 1.44 eV, and the X-W lineup is 0.84 eV. Both of these estimates are in reasonably good agreement with our calculations, but not with the experimental results. One possible conclusion is that the Al band structure simply cannot be described accurately by a weak empirical pseudopotential model, even over a limited range of energies near the Fermi surface.

The quasiparticle bandwidth for Al is found to be 10.0 eV. This is 0.6 eV (about 6%) smaller than experiment. Some of the discrepancy may result from the plasmon-pole approximation, which, as discussed in Sec. V, tends to overestimate the bandwidth narrowing for systems with $r_s \simeq 2$. A more accurate approximation for the q dependence of K_{xc}, also discussed into Sec. V, may lead to better agreement.

The general trend in the self-energy correction versus energy is illustrated in Fig. 1 for the three metals. The self-energy correction is found to be, for the most part, a linear function of energy with very little scatter. The shape of these plots is very different from the corresponding plots for the semiconductors Si and Ge, where local-field effects are important. In Ge and Si the energy dependence of the self-energy correction is dominated by a ~0.7-eV discontinuity occurring between the valence and conduction bands. We found that local-field effects have very little effect on the quasiparticle energies for the alkali metals.[12]

V. ANALYSIS OF RESULTS AND SYSTEMATIC TRENDS

In the preceding section complete results have been given for the quasiparticle spectrum of Li, Na, and Al. Here, we wish to understand several aspects of these results: (i) the validity of the plasmon-pole model, (ii) the validity of the LDA for K_{xc}, (iii) the role of the crystalline potential in the self-energy; (iv) a simple explanation for the density dependence of the bandwidth reduction, (v) the behavior of the screened-exchange and Coulomb-hole parts of the self-energy, (vi) density-of-states mass enhancements due to correlation, and (vii) comparison to other schemes for including correlation effects in simple metals. For this purpose, the homogeneous electron gas (jellium) is quite convenient. There are no crystal-potential or local-field effects. This renders the calculation using the present scheme straightforward. Also,

most previous calculations of correlation effects in metals have been performed for the jellium model.

For the electron gas, the self-energy can be written in the same approximation as used above:

$$\Sigma(\mathbf{k})=-\sum_{\mathbf{q}} v(\mathbf{q})n(\mathbf{k}-\mathbf{q})(1+\omega_p^2/\{[E(\mathbf{k})-E(\mathbf{k}-\mathbf{q})]^2-\tilde{\omega}^2(q)\})+\sum_{\mathbf{q}} v(\mathbf{q})[\omega_p^2/2\tilde{\omega}(\mathbf{q})]/[E(\mathbf{k})-E(\mathbf{k}-\mathbf{q})-\tilde{\omega}(\mathbf{q})] , \tag{13}$$

where $\tilde{\omega}(\mathbf{q})$ is an effective plasma frequency given by the f-sum rule,[4] $v(\mathbf{q})$ is the bare Coulomb interaction, ω_p is the plasma frequency at $\mathbf{q}=\mathbf{0}$, $n(\mathbf{k})$ is the electron occupation number, and $E(\mathbf{k})$ is the quasiparticle energy. The first term is the screened exchange (SX) and the second is the Coulomb hole (CH). Since $E(\mathbf{k})$ itself depends on Σ, an iterative procedure is required to determine E and Σ. In the present plasmon-pole model for the electron gas, the static dielectric function determines the $\mathbf{q}$ dependence of the effective plasma frequency:

$$\tilde{\omega}^2(\mathbf{q})=\omega_p^2/[1-\epsilon^{-1}(\mathbf{q})] . \tag{14}$$

This result for the effective plasmon frequency was first employed by Overhauser.[23] This is a special case of the general result employed in the calculations for the inhomogeneous systems.

A. Accuracy of the plasmon-pole model

We have tested the validity of the plasmon-pole model by comparison to Hedin's original self-energy calculations, in which the ω dependence of the RPA (Lindhard) dielectric function was employed. To make a meaningful comparison, we must employ the RPA static dielectric function as well as the free-electron spectrum, rather than the self-consistent quasiparticle spectrum, in the Green function. The free-electron spectrum must be shifted by a constant amount so that the free-electron and quasiparticle Fermi levels are coincident. Results for the bandwidth corrections obtained with these two methods are given in Table IV and Fig. 2. The plasmon-pole approximation is seen to be very good in the region $r_s>2$. Also listed in Table IV are results obtained by Lundqvist with use of a different plasmon-pole dielectric function.[24] However, unlike ours, this dielectric function does not reduce to the RPA dielectric function in the static limit and, consequently, those results are slightly different from ours.

B. Different approximations for K_{xc}

In order to determine the sensitivity of the calculated quasiparticle spectrum to the approximations employed for K_{xc}, we have carried out self-energy calculations with several different dielectric functions including the LDA, RPA, and the Singwi-Sjölander-Tosi-Land (SSTL) dielectric functions.[25] The LDA dielectric function corresponds to a constant ($\mathbf{q}$ independent) K_{xc}. The constant depends on r_s. The RPA dielectric function corresponds to $K_{xc}=0$. The SSTL dielectric function corresponds to a q-dependent K_{xc} of the form

$$K_{xc}^{SSTL}(q)=-av(q)[1-\exp(-bq^2/k_F^2)] . \tag{15}$$

The parameters a and b depend on r_s and were obtained from numerical calculations of the dielectric function including many-body effects.[25] A Hubbard form for the dielectric function was also considered:

$$K_{xc}^{Hubbard}(q)=K_{xc}^{LDA}k_F^2/(k_F^2+q^2) . \tag{16}$$

The static dielectric functions studied here are plotted in Fig. 3 for the electron gas (with $r_s=4$). The renormalized Hubbard and SSTL dielectric functions have values which lie between the LDA and RPA curves. A static perturbation in the electron gas is more completely screened by the LDA dielectric function than with the RPA function. Corresponding to this more effective screening, the effective plasma frequency [given by Eq. (14)] obtained from the LDA dielectric function is significantly smaller than the RPA effective plasma frequency. From Eq. (13) we see that a reduction in the effective plasma frequency increases the strength of the coupling between the electrons and plasmons. Thus, the

TABLE IV. Test of the accuracy of the plasmon-pole approximation for the electron gas. The bandwidth correction (in eV) is calculated for several different values of electron density (r_s). Calculations do not include an updated quasiparticle spectrum in the Green function. Hedin's results are obtained with the full frequency-dependent Lindhard dielectric function. Other results are obtained with plasmon-pole dielectric functions as described in the text.

	r_s				
	1	2	3	4	5
Lindhard (Hedin)	0.99	−0.29	−0.33	−0.27	−0.23
Plasmon pole (Lundqvist)	1.18	−0.08	−0.18	−0.16	−0.14
Plasmon pole (present)	−0.04	−0.41	−0.31	−0.23	−0.18

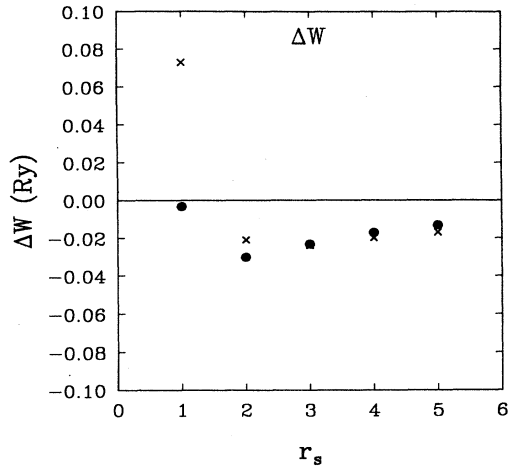

FIG. 2. Many-body correction ΔW to the free-electron bandwidth plotted as a function of r_s. Crosses indicate bandwidth corrections calculated by Hedin (Refs. 6 and 7) with the full ω-dependent RPA dielectric function. Solid circles indicate the corrections calculated here with the RPA plasmon-pole dielectric function. The plasmon-pole dielectric function gives ΔW in good agreement with that obtained with the full ω-dependent RPA dielectric function for $r_s \geq 2$.

self-energy corrections obtained with the LDA dielectric function are larger than those obtained with the RPA dielectric function.

Table V contains the calculated corrections to the free-electron bandwidth for $2 < r_s < 5$. The SSTL and LDA functions give similar corrections over the entire range considered. The renormalized Hubbard function gives slightly smaller bandwidth corrections. For example, the renormalized Hubbard function gives a self-energy correction that is smaller than that obtained with the LDA function by 0.1 eV for $r_s = 4$. Thus the bandwidth correction is not very sensitive to the q dependence of K_{xc}.

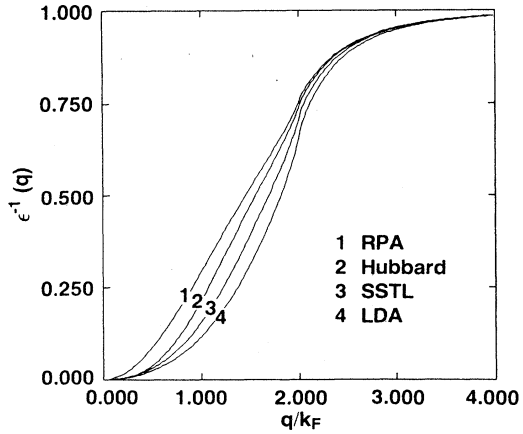

FIG. 3. Inverse static dielectric functions (see text) plotted as a function of q/k_F. Plots are for $r_s = 4$.

TABLE V. Electron-gas results for the bandwidth correction ΔW, the Fermi-level mass enhancement $1+\lambda$, and the renormalization constant $Z(k_F)$. Results are obtained using four different static dielectric functions (i.e., different K_{xc}).

Dielectric function	r_s	ΔW (eV)	$1+\lambda$	$Z(k_F)$
RPA ($K_{xc}=0$)				
	2	−0.56	0.994	0.775
	3	−0.46	1.026	0.703
	4	−0.35	1.060	0.646
	5	−0.25	1.075	0.601
$K_{xc}=K_{xc}^{LDA}$				
	2	−1.17	1.028	0.757
	3	−0.86	1.092	0.672
	4	−0.64	1.163	0.602
	5	−0.51	1.247	0.539
$K_{xc}=K_{xc}^{Hubbard}$				
	2	−0.95	1.016	0.765
	3	−0.72	1.066	0.688
	4	−0.54	1.121	0.626
	5	−0.44	1.176	0.573
$K_{xc}=K_{xc}^{SSTL}$				
	2	−1.20	1.029	0.758
	3	−0.84	1.087	0.677
	4	−0.61	1.150	0.612
	5	−0.46	1.197	0.560

C. Role of the crystal potential

The results obtained here for the occupied bandwidth reductions in the electron gas are very close to those obtained in the calculations employing the crystal Green function and the full dielectric matrix. This suggests that we can obtain meaningful comparisons to experiment by adding the corrections determined for the electron gas to the LDA bandwidths. For Na, with $r_s = 3.95$, we obtain an occupied valence bandwidth of 2.52 eV; for Li, with $r_s = 3.25$, we obtain 2.65 eV; and for Al, with $r_s = 2.07$, we obtain 9.90 eV. These values are all within 0.2 eV of the results obtained in the full calculations and deviate from experiment by 3% for Na, 12% for Li, and 7% for Al. For Li the comparison with experiment is somewhat less meaningful because the crystal potential has a relatively more important effect on the Green function and the dielectric function. In this sense, the free-electron model is better for Na and Al than for Li.

D. Bandwidth correction: Dependence on electron density

The dependence on electron density of several aspects of correlation effects in the electron gas are given by Hedin and Lundqvist.[7] Here we focus on the correction to the occupied bandwidth. This is illustrated in Fig. 2 for the case of RPA screening. For intermediate density, ΔW is negative and of order -0.25 eV. With decreasing density it tends to zero. In the high-density limit, ΔW is positive, with the crossover occurring for $1 < r_s < 2$ in the work of Hedin. As noted above, for $r_s > 2$ the present

plasmon-pole model follows the full dynamical RPA calculation. The inclusion of K_{xc} systematically enhances ΔW in that range of r_s.

In the simplest terms the systematic trends for ΔW result from the competition between the SX and CH terms in Σ. From Eq. (13) the CH term has precisely the form of the self-energy of the large-polaron problem (weak coupling). In accordance with that analogy, the CH term enhances the mass, and hence reduces W. This is purely a dynamical effect; the CH term is k independent in the static COHSEX approximation discussed by Hedin. The bare-exchange term obviously increases W. For $\mathbf{q}$ near zero in Eq. (13) there is twice as much available phase space for $k=0$ as for $k=k_F$. This causes the bare-exchange term to be larger in magnitude for $k=0$ than for $k=k_f$, and leads to an increase in W. In the static approximation, the screened-exchange term corresponds to replacing $v(q)$ with $\epsilon^{-1}(\mathbf{q})v(\mathbf{q})$ in the Hartree-Fock expression for bare exchange. Thus, the range of the statically screened Coulomb interaction is determined by the Thomas-Fermi wave vector q_{TF}. The magnitude of the effect of including screening depends on whether $q_{TF}>k_F$ or $q_{TF}<k_F$. In the former case ($r_s>1.5$), $\epsilon^{-1}(q)v(q)\simeq 0$ over most of the Fermi sphere; thus the SX term is suppressed. In the latter case ($r_s<1.5$) screening is ineffective and the bare-exchange result pertains. This is the qualitative reason for the crossover in sign for ΔW near $r_s\simeq 1.5$ in Hedin's RPA results. Dynamical effects complicate this picture of SX as noted below.

E. Momentum decomposition of screened-exchange and Coulomb-hole parts of the self-energy

For the range of r_s covered by Al, Li, and Na, a large fraction of the bandwidth reduction results from the fact that the Coulomb-hole contribution to the self-energy is negative and increases in magnitude (monotonically) as k is increased from $k=0$ to $k=k_F$. The bandwidth correction arising from the SX term is typically somewhat smaller than that from the CH term, and can be positive or negative depending on the q dependence of the static dielectric function. With the RPA dielectric function the SX term increases the bandwidth by a small amount, but with the LDA dielectric function the SX term leads to a reduction in the bandwidth. With the LDA dielectric function the CH term contributes -0.44 eV and the SX term contributes -0.21 eV to the difference $\Sigma(k_F)-\Sigma(0)$ for $r_s=4$. With the RPA dielectric function the CH term contributes -0.36 eV and the SX term contributes 0.01 eV.

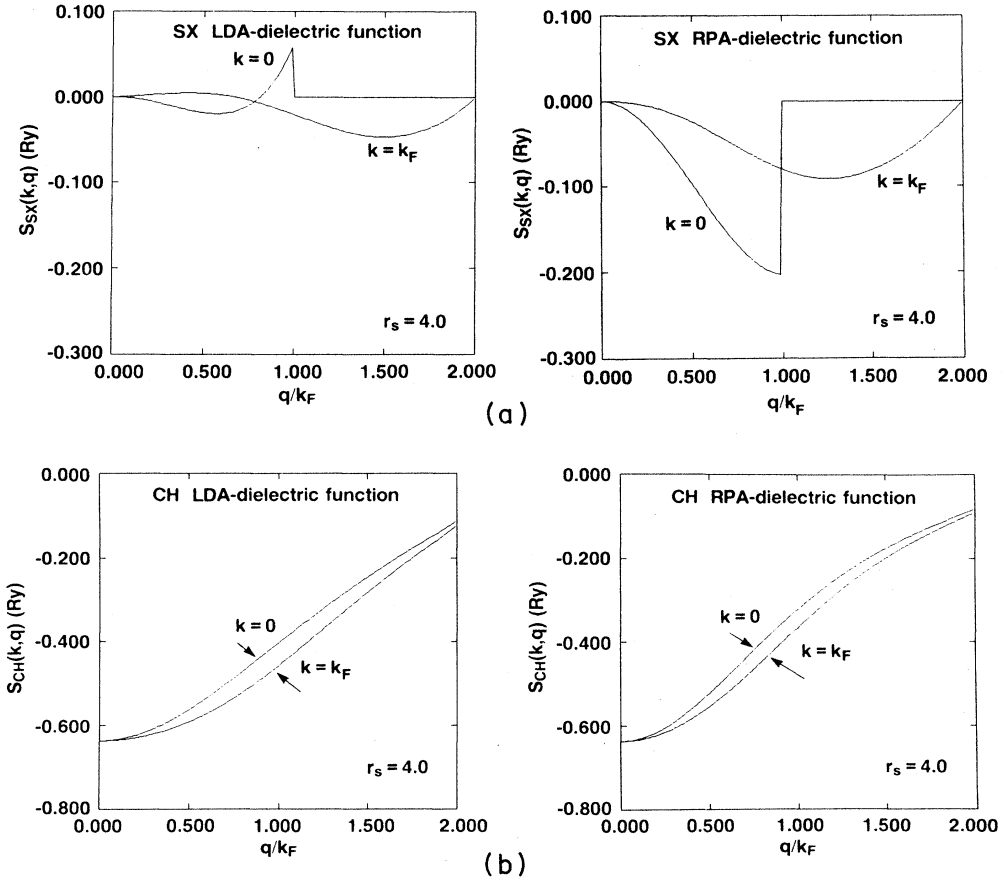

FIG. 4. Momentum decomposition for the screened-exchange (SX) and Coulomb-hole (CH) terms in the self-energy for $k=0$ and k_F. Plots correspond to $r_s=4$. Results obtained with both the RPA and LDA dielectric functions are plotted. The area between the curves is the bandwidth correction.

The self-energy can be written in terms of an integration over momentum transfer q:

$$\Sigma(k)=\int [S_{\rm SX}(k,q)+S_{\rm CH}(k,q)]dq \ . \tag{17}$$

The functions $S_{\rm SX}$ and $S_{\rm CH}$ are plotted in Fig. 4 for $k=0$ and k_F for both the RPA and LDA dielectric functions. The bandwidth reduction is just the area between the curves for $k=k_F$ and 0. With the RPA dielectric function there is a nearly complete cancellation between the contributions from the regions $0<k<k_F$ and $k>k_F$. Thus the SX term contributes very little to the bandwidth reduction in the RPA for $r_s=4$. This cancellation is somewhat less complete when the LDA dielectric function is employed. It should be noted that the screened-exchange contribution for $k=0$ depends rather sensitively on the screening. The function $S_{\rm SX}(0,q)$ can be written

$$S_{\rm SX}(0,q)=-(4/\pi)(1+\omega_p^2/\{[E(q)-E(0)]^2-\tilde{\omega}^2(q)\})\Theta(k_F-q) \ . \tag{18}$$

A singularity will occur at q_s if the quasiparticle energy difference $E(q_s)-E(0)$ becomes equal to the effective plasmon energy $\tilde{\omega}(q_s)$ for a value of $q_s<k_F$. Clearly, $q_s>k_F$ in both cases shown in Fig. 4(a), but with the LDA dielectric function q_s is nearer to k_F and an increase in $S_{\rm SX}$ occurs as q approaches k_F. Of course, the validity of the plasmon-pole approximation requires $q_s>k_F$.

As noted, the CH term can be interpreted as the interaction energy, calculated with second-order perturbation theory, of a single electron with the plasmons. It is larger in magnitude (more negative) for $k=k_F$ than for $k=0$ because, for a given $|\mathbf{q}|$, the energy denominator $E(\mathbf{k})-E(\mathbf{k}-\mathbf{q})-\tilde{\omega}(\mathbf{q})$ is, on the average, smaller in magnitude for the intermediate states available to an electron with $k=k_F$ than to one with $k=0$. In physical terms this corresponds to a greater probability for a moving electron to emit and reabsorb a virtual plasmon than for one at rest. The strength of the effective electron-plasmon interaction is inversely proportional to $\tilde{\omega}(\mathbf{q})$, and the CH contribution is larger with the LDA dielectric function than with the RPA dielectric function because $\tilde{\omega}(\mathbf{q})$ is smaller.

F. Fermi-level density-of-states enhancement

Other interesting quasiparticle properties include the density of states (effective mass) at the Fermi level and the discontinuity in the momentum distribution at the Fermi surface $[Z(k_F)]$. The effective-mass enhancement due to exchange correlation, $m^*=(1+\lambda)m_0$, and $Z(k_F)$ have been calculated using the present approach for the electron gas. The results for $1+\lambda$ and $Z(k_F)$ are shown in Table V, with and without $K_{\rm xc}$ in the screening. Clearly, the LDA dielectric function gives a significantly larger λ than the RPA dielectric function. The calculated values of $1+\lambda$ are sensitive to the form of $K_{\rm xc}$. Comparison with heat-capacity measurements and estimates for the electron-phonon contribution to λ indicate that the electron-gas results in Table V overestimate λ due to electron-electron interactions. For example, in K, $1+\lambda_{e\text{-}e}\simeq 1.09\pm 0.03$ as measured and corrected for $\lambda_{e\text{-ph}}$. For $r_s=5$ our theoretical results fall in the range 1.18–1.25 depending on the form of $K_{\rm xc}$. For Na the corresponding experimental result is $1+\lambda_{e\text{-}e}\simeq 1.09\pm 0.04$. For $r_s=4$ our results fall in the range 1.12–1.16. This disagreement may be due to several possibilities. First, the plasmon-pole model may be too crude to describe the Fermi-surface properties if they depend on the details of the low-energy excitations near the Fermi level. Second, the present results for λ are strongly influenced (as much as a factor of 2) by the self-consistent update of the quasiparticle spectrum. Thus a very precise treatment of the energy dependence of the Green function, especially near the Fermi energy, may be important for obtaining the correct mass enhancements. Precise calculation of the Fermi-surface properties for the alkali metals requires treating the electron-phonon interaction, the electron-electron interaction, and ordinary band-structure effects on equal footing, and remains an open problem.

G. Comparison to other theoretical work

In most early studies emphasis was placed on Fermi-surface properties.[26] More recently, some work has been done on the bandwidth, in the context of the jellium model. The early work of Hedin is summarized in Fig. 2 and Table IV. In Table VI we compare our results to those of Ng and Singwi[27] and Zhu and Overhauser.[11] Both of these calculations include coupling to spin fluctuations in

TABLE VI. Comparison of $m_{\rm av}/m$ to other theoretical work.

	r_s					
	2	3	4	5	6	
Ng and Singwi	0.98	1.02	1.06	1.10	1.14	
Present[a]	1.095	1.168	1.234	1.296	1.352	
	r_s					
	2.07	3.25	3.93	4.87	5.12	5.62
Zhu and Overhauser	1.171	1.337	1.334	1.260	1.231	1.170
Present[a]	1.101	1.185	1.230	1.287	1.302	1.331

[a]These results obtained with exchange only, $K_{\rm xc}$; $K_{\rm xc}=-2\pi/k_F^2$.

addition to the density fluctuations, but using rather different models. Ng and Singwi relate the self-energy approximately to the irreducible particle-hole interaction, which is, in turn, identified with the "local fields" (in the sense of short-range correlations in the screening). The corresponding local-field correction $G(q)$ is approximated along the lines of the original Hubbard model. Zhu and Overhauser extend the one-plasmon-pole model to include a paramagnon branch of excitations. The results for available values of r_s are compared in Table VI where the average mass enhancement ($m_{\rm av}/m = k_F^2/W$) is shown. The present approach yields significantly more reduction in the bandwidth than does that of Ng and Singwi. The systematic trend in $m_{\rm av}/m$ versus r_s is rather different in comparison to Zhu and Overhauser, the latter showing a maximum near $r_s \simeq 4$. They obtain a bandwidth reduction of 0.83 eV for a free-electron gas of $r_s = 3.93$, a reduction of 1.20 eV for $r_s = 3.25$, and one of 1.69 eV for $r_s = 2.07$. Keeping in mind that the correlation effect on W in these simple metals is essentially independent of the crystal potential, we can reduce the LDA bandwidths by these corrections. Thus with the model of Zhu and Overhauser, one obtains widths of 2.33 eV for Na, 2.25 eV for Li, and 9.38 eV for Al. Compared to experiment, these are too small by about 12% for Na, 25% for Li, and 11% for Al. On the other hand, Ng and Singwi obtain reductions which are systematically too small.

Shung, Sernelius, and Mahan[28] have adopted a somewhat different approach to explain the narrowing of the Na bandwidth. While they include self-energy corrections, similar in magnitude to those given by Hedin, they also argue that the photoemission process itself yields an apparent narrowing of the bandwidth. They find that the measured valence-band width should depend on the range of photon energies employed in the photoemission experiments. However, no such dependence is seen in the experiments.[8] A more accurate determination of the effect of the surface on the measured photoemission spectrum of Na may require a calculation of the self-consistent surface potential, including atomic relaxation.

VI. CONCLUSIONS

We have shown that it is possible to calculate accurate quasiparticle band structures for simple metals with use of the GW formalism of Hedin and the plasmon-pole model. In general, the calculated energies are in excellent agreement with experimental data from photoemission[8–10,21] and soft-x-ray–emission[19] experiments. The one exception is the X_1-point energy in Al, for which a 0.35-eV difference between theory and experiment still exists. The theoretical method employed here also gives accurate quasiparticle excitation energies for semiconductors and insulators.[4] Thus, the GW formalism is valid for systems varying from nearly-free-electron low-density metals, such as Na, to high-electron-density insulators, such as C, which have highly inhomogeneous charge distributions. For the low-density metals studied here, inclusion of exchange-correlation effects in the dynamic dielectric function is shown to be important. However, for the simple metals, local-field effects, resulting from inhomogeneous charge densities, are very small.

ACKNOWLEDGMENTS

This work was initiated while two of us (J.E.N. and M.S.H.) were at the University of California, Berkeley. The work done at the University of California, Berkeley, was supported by the National Science Foundation (NSF) under Grant No. DMR-88-18404 and by the Director, Office of Energy Research, Office of Basic Energy Sciences, Materials Science Division of the U.S. Department of Energy under Contract No. DE-AC03-76SF00098. A grant of Cray computer time at the NSF San Diego Supercomputer Center (GA Technologies, Inc.) is gratefully acknowledged.

[1]W. Kohn and L. J. Sham. Phys. Rev. **140**, A1133 (1965).
[2]M. S. Hybertsen and S. G. Louie, Comments Condensed Mater. Phys. **13**, 223 (1987), and references therein.
[3]E. W. Plummer, Surf. Sci. **152/153**, 162 (1985).
[4]M. S. Hybertsen and S. G. Louie, Phys. Rev. Lett. **55**, 1418 (1985); Phys. Rev. B **34**, 5390 (1986).
[5]R. W. Godby, M. Schlüter, and L. J. Sham, Phys. Rev. Lett. **56**, 2415 (1986); Phys. Rev. B **35**, 4170 (1987); **37**, 10 159 (1988).
[6]L. Hedin, Phys. Rev. **139**, A796 (1965).
[7]L. Hedin and S. Lundqvist, in *Solid State Phyiscs,* edited by F. Seitz and D. Turnbull (Academic, New York, 1968), Vol. 23, p. 1.
[8]E. Jensen and E. W. Plummer, Phys. Rev. Lett. **55**, 1918 (1985).
[9]I. Lyo and E. W. Plummer, Phys. Rev. Lett. **60**, 1558 (1988).
[10]S. P. Kowalczyk, L. Ley, F. R. McFeely, R. A. Pollak, and D. A. Shirley, Phys. Rev. B **8**, 3583 (1973).
[11]X. Zhu and A. W. Overhauser, Phys. Rev. B **33**, 925 (1986).
[12]J. E. Northrup, M. S. Hybertsen, and S. G. Louie, Phys. Rev. Lett. **59**, 819 (1987).
[13]P. Singhal and J. Callaway, Phys. Rev. B **14**, 2347 (1976); M. S. Hybertsen and S. G. Louie, *ibid.* **35**, 5585 (1987).
[14]G. Strinati, H. Mattausch, and W. Hanke, Phys. Rev. B **25**, 2867 (1982).
[15]The correlation energy used is from D. M. Ceperley and B. J. Alder [Phys. Rev. Lett. **45**, 566 (1981)] as parametrized by J. P. Perdew and A. Zunger [Phys. Rev. B **23**, 5048 (1981)].
[16]G. P. Kerker, J. Phys. C **13**, L189 (1980).
[17]J. Ihm, A. Zunger, and M. L. Cohen, J. Phys. C **12**, 4409 (1979).
[18]D. J. Chadi and M. L. Cohen, Phys. Rev. B **8**, 5747 (1973).
[19]R. S. Crisp and S. E. Williams, Philos. Mag. **5**, 1205 (1960).
[20]P. H. Citrin, G. K. Wertheim, T. Hashizume, F. Sette, A. A. Macdowell, and F. Comin, Phys. Rev. Lett. **61**, 1021 (1988).
[21]H. J. Levinson, F. Greuter, and E. W. Plummer, Phys. Rev. B **27**, 727 (1983).
[22]The Z point is defined here to be the point half-way between X and W. See Fig. 8 of Ref. 21.
[23]A. W. Overhauser, Phys. Rev. B **3**, 1888 (1971).
[24]B. I. Lundqvist. Phys. Kondens. Mat. **6**, 206 (1967).

[25]K. S. Singwi, A. Sjölander, M. P. Tosi, and R. H. Land, Phys. Rev. B **1**, 1044 (1970).

[26]A. H. McDonald, M. W. C. Dharma-wardana, and D. J. W. Geldart, J. Phys. F **10**, 1719 (1980); A. H. McDonald, *ibid.* **10**, 1737 (1980).

[27]T. K. Ng and K. S. Singwi, Phys. Rev. B **34**, 7738 (1986); **34**, 7743 (1986).

[28]K. W.-K. Shung, B. E. Sernelius, and G. D. Mahan, Phys. Rev. B **36**, 4499 (1987).